JACS
JOURNAL OF THE AMERICAN CHEMICAL SOCIETY
Article
pubs.acs.org/JACS

Pasteur's Tweezers Revisited: On the Mechanism of Attrition-Enhanced Deracemization and Resolution of Chiral Conglomerate Solids

Jason E. Hein,[†,‡] Blessing Huynh Cao,[‡] Cristobal Viedma,[§] Richard M. Kellogg,[⊥] and Donna G. Blackmond*[,†]

[†]Department of Chemistry, The Scripps Research Institute, La Jolla, California 92037, United States
[‡]Department of Chemistry, University of California, Merced, California 95344, United States
[§]Departamento Crystalografia-Mineralogia, Facultad Geologia, Universidad Complutense, 28040 Madrid, Spain
[⊥]Syncom BV, Kadijk 3, 9747 AT Groningen, The Netherlands

Supporting Information

ABSTRACT: Insights into the mechanism of attrition-enhanced deracemization and resolution of solid enantiomorphic chiral compounds are obtained by crystal size and solubility measurements and by isotopic labeling experiments. Together these results help to deconvolute the various chemical and physical rate processes contributing to the phenomenon. Crystal size measurements highlight a distinct correlation between the stochastic, transient growth of crystals and the emergence of a single solid enantiomorph under attrition conditions. The rapid mass transfer of molecules between the solution and solid phases under attrition is demonstrated, and the concept of a crystal-size-induced solubility driving force is exploited to overcome the stochastic nature of the crystal growth and dissolution processes. Extension to non-racemizing conditions provides a novel methodology for chiral resolution. Implications both for practical chiral separations and for the origin of biological homochirality are discussed.

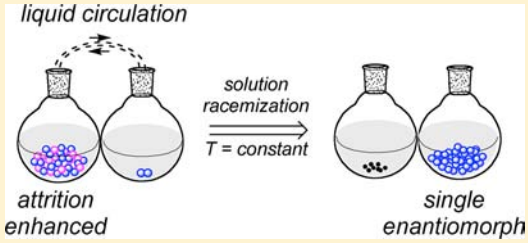

INTRODUCTION

Ever since Viedma's[1] striking demonstration that attrition of a racemic slurry of enantiomorphic solids promotes an inexorable emergence of solid-phase homochirality, this phenomenon has been the subject of intense interest from both practical and fundamental perspectives. The phenomenon was initially applied to molecules such as $NaClO_3$ that are achiral in solution but exist as two mirror-image solids, or enantiomorphs, and whose phase behavior has intrigued scientists from the time of van't Hoff.[2,3] The idea that this concept could be extended to intrinsically chiral molecules that can be made to interconvert in solution (Scheme 1) was recently realized,[4,5] and implications for the evolution of biological homochirality from a racemic prebiotic mixture of enantiomers have been discussed.[4−10]

Scheme 1. Evolution of Solid-Phase Homochirality from a Mixture of Racemizable Chiral Conglomerate Crystals

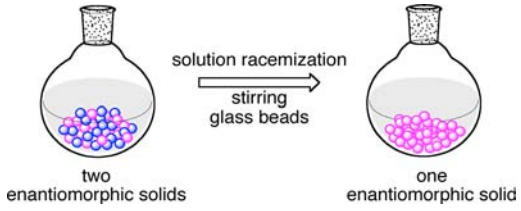

The potential for development of an efficient separation/deracemization methodology in a pharmaceutical context has also been noted.[8] For example, slurry mixtures of compound **1**, a conglomerate imine derivative of 2-Cl-phenylglycine, the (*S*) enantiomer of which makes up the chiral component of the blockbuster drug Clopidogrel (Plavix), undergoes interconversion between the two enantiomorphic solids with vigorous stirring under attrition or sonication in the presence of an organic base (Scheme 1). This system has been studied extensively in detailed mechanistic and scale-up studies of the attrition-enhanced deracemization process.[11]

At the same time, ongoing research seeks a better understanding of the physical and chemical processes underlying the phenomenon. In addition to further experimental studies on a variety of systems,[11,12] several types of mathematical models have been presented, including Monte Carlo simulations of the process[13] and kinetic modeling of

Received: April 13, 2012
Published: July 10, 2012

   dx.doi.org/10.1021/ja303566g | J. Am. Chem. Soc. 2012, 134, 12629−12636

reaction-type networks.[14] A recent report[15] based on population balance modeling helps to overcome limitations of these earlier efforts by providing a more accurate mathematical description of the processes thought to be involved in the deracemization, including solution racemization, crystal attrition and agglomeration, and crystal growth and dissolution caused by crystal-size dependence of solubility.

It is generally accepted that the deracemization mechanism requires (i) chemical racemization in solution, (ii) crystal growth, and (iii) mechanical or thermal energy input to instigate crystal dissolution, typically attrition by grinding. The latter two are physical processes that influence the solubility of the system as dictated by the Gibbs−Thomson rule (larger crystals exhibit lower solubility than smaller crystals). Crystal growth occurs by Ostwald ripening (growth of larger crystals at the expense of smaller crystals), and mechanical grinding or sonication enhances crystal attrition. When enantiomorphic crystals of a chiral molecule are mixed together as a slurry in the presence of a racemization catalyst, these chemical and physical processes combine to allow the system to evolve to a single solid enantiomorph. A central mechanistic question that has been posed is whether attrition-enhanced deracemization may be rationalized by consideration of solubility and crystal growth stemming from tenets of the Gibbs−Thomson rule, as was originally proposed by Viedma[7] and by Blackmond,[8] or whether additional driving forces are required to explain the temporal evolution of solid-phase enantiomeric excess (ee).

In this report we present experimental results that help in deconvolution of the various chemical and physical rate processes that occur during attrition-enhanced deracemization. Careful solubility and crystal size measurements offer evidence for the role of crystal-size-induced solubility differences over the course of the deracemization process. Isotopic labeling aids in the deconvolution of the physical mass transfer from the net conversion of molecules from one enantiomorph to the other. This work provides further insights into the mechanism of attrition-enhanced deracemization and resolution of chiral conglomerate solids and proposes a novel modification of the protocol for practical and reproducible chiral separations.

RESULTS AND DISCUSSION

Effect of Crystal Size on Deracemization. Attrition-enhanced deracemization was carried out by sonication of racemic mixtures of compound **1** in MeCN in the presence of glass beads, using catalytic 1,8-diazabicyclo[5.4.0]undec-7-ene (DBU) to induce solution-phase racemization. Crystal enantiomeric excess (%CEE) was monitored over time for 24 experiments monitored for up to 22 h. Figure 1 shows the results of experiments carried out under apparently identical conditions and underscores the variability of the outcome: the 24 runs produced nine cases of homochiral *R*-**1**, eight of homochiral *S*-**1**, and seven that remained racemic. The time required for the evolution of solid-phase ee and the form of the profile differed even for seemingly identical initial conditions.[16]

The apparent randomness of the deracemization process for equal initial masses of two enantiomorphic crystals has been reported previously.[12] By contrast, however, the mathematical model reported by Iggland and Mazzotti[15] demonstrated that, in a system exhibiting perfect initial symmetry, symmetry will be conserved. These authors suggested that the observation of apparent randomness instead may indicate either the existence of undetectable initial asymmetry in crystal size or CEE, or alternatively the presence of trace chiral impurities. In the present work, the nearly equal number of conversions to opposite enantiomorphs suggests that any influence from chiral impurities is small.[17] It is important to note that the outcome of the mathematical model is sensitive to the specific parameter values chosen and to the particular rules employed for how crystals break and how crystals grow. In addition, the model does not account for any variability in how these physical processes occur under actual experimental conditions. Thus, it is reasonable to assume not only that identical initial conditions of mass and crystal size distribution may be difficult to achieve experimentally, but also that, under macroscopic experimental attrition conditions, not all crystal-breaking events for any given crystal size occur in an identical manner, as they do in the mathematical model. This factor may help account for differences in the temporal profiles for evolution of solid-phase homochirality as well as the apparent randomness in the sense of the outcome shown in Figure 1.

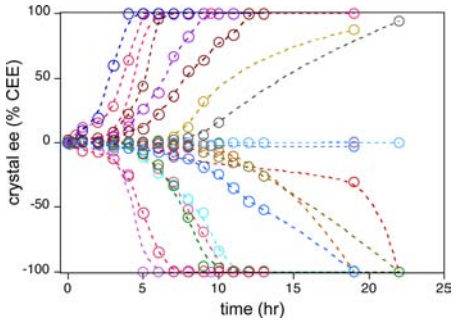

Figure 1. Evolution of solid-phase enantiomeric excess (%CEE) of *rac*-**1** over time during 24 attrition-enhanced deracemization experiments carried out under identical conditions. Dotted lines are given as a guide to the eye.

Three of the experiments from Figure 1 are analyzed in further detail in Figures 2 and 3. Two of the three experiments achieved solid-phase homochirality—in opposite senses—in an accelerated manner within 5 h, while the third sample remained racemic even after 10 h (Figure 1). Crystal size distributions were measured for all three experiments at times designated by arrows in Figure 2, namely at the outset of the deracemization experiment and after 3, 5, and 8 h.[18] Although the three samples exhibit similar, non-Gaussian crystal size distributions at the outset, intriguingly, it was found that a broadening of the distribution commenced at the onset of the evolution of solid-phase CEE at 3 h and endured through the emergence of homochirality at ca. 5 h for series b and series c (Figure 2). By contrast, the sample that remained racemic (series a) retained a narrow size distribution and smaller average size throughout the grinding/sonication process. In addition, Figure 2 shows that, after the system converts to a single solid enantiomorph, further attrition returns the system to its original crystal size distribution. Thus, a transient growth in crystal size is implicated in the accelerating profile for the evolution of solid-phase homochirality. The crystals are irregularly shaped, as shown in Figure 3, and their size is calculated as the rectangular crystal area as defined by the two-dimensional perimeter, as is common practice in measurements of biological samples.[19] This deviation from ideal spherical crystals may also rationalize differences between experimental %CEE profiles and that predicted for ideal spherical crystals in mathematical models such as ref 15.

The link between an increasing crystal size and the evolution of solid-phase homochirality is in accord with the original

dx.doi.org/10.1021/ja303566g | J. Am. Chem. Soc. 2012, 134, 12629−12636

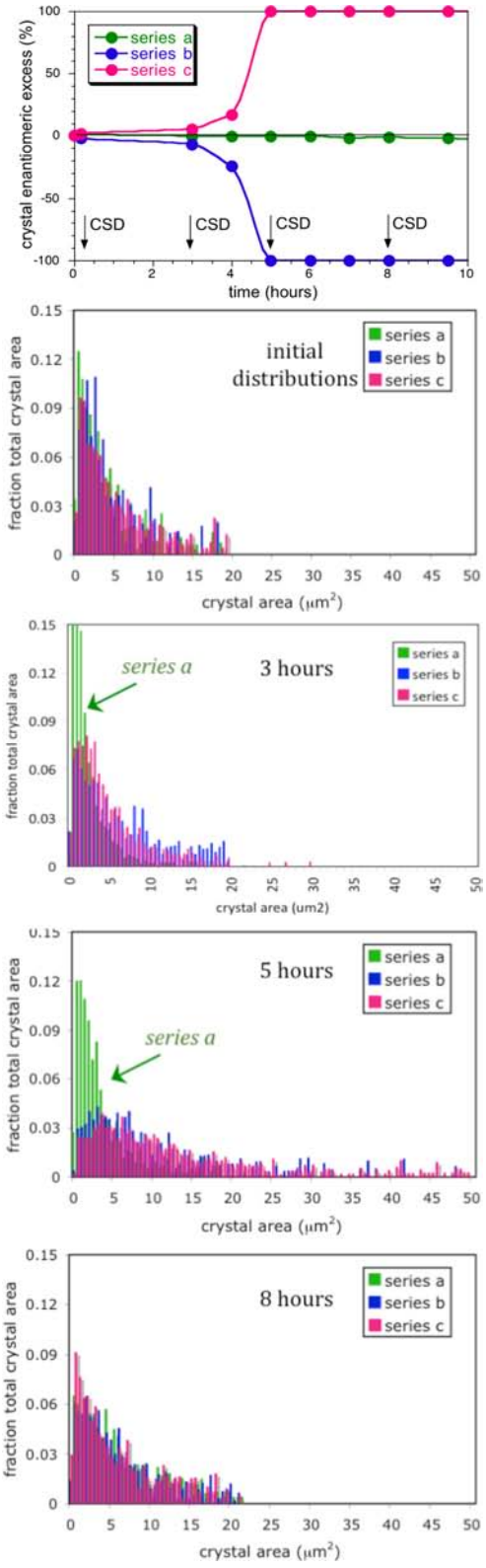

Figure 2. %CEE curves of three attrition-enhanced deracemization experiments (top) and crystal area distributions (bottom) measured for solid-phase samples at the time points noted by arrows (top). Crystal size distribution (CSD) is measured as the two-dimensional surface area of the non-spherical crystals.[16]

proposals of the Gibbs–Thomson rule for crystal size-dependent solubility and Ostwald ripening as the driving mechanism behind the deracemization process. A ca. 10% lower

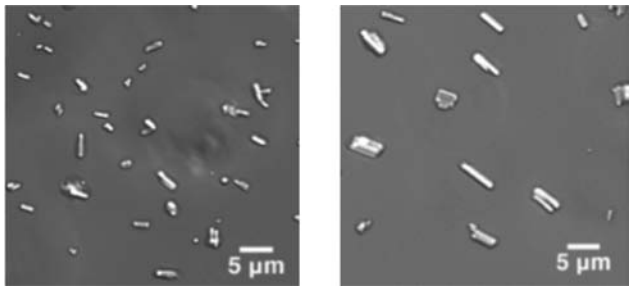

Figure 3. Optical microscopy showing crystals from series a (left) and series b (right) after 5 h of enhanced attrition/deracemization, from which the crystal size distributions shown in the middle of Figure 2 were determined.[16]

solubility was measured in slurries of crystals in the larger size range (shown in Figure 2 after 5 h) compared to those with the initial narrower distribution, as is predicted by the Gibbs–Thomson rule. For series b and series c in Figure 2, the smaller crystals dissolve and feed the growing larger crystals as predicted by Ostwald ripening. In these cases the movement from small to large crystals is accompanied by a net movement of mass from one enantiomorph to the other via the conduit of solution-phase racemization. The experimental results do not reveal why crystal growth occurred in these two cases nor in the third, but these observations imply that the deracemization process is instigated by what might be considered an "internal seeding" event whereby larger crystals are stochastically formed and temporarily sustained during a period of rapid mass movement from one enantiomorph to the other estimated at ca. 1 mg/min during this critical period.[18] This suggests that the accelerated deracemization rate is limited by the rate at which molecules are able to dissolve from the enantiomorph being depleted. A net movement of molecules from small to large crystals is set up by this temporary perturbation of the reversible physical equilibrium of the dissolution process. The driving force of net dissolution for small crystals together with the thermodynamic driving force of crystal growth provide self-reinforcing effects that rationalize the autoinductive profile of crystal ee vs time.

Such a perturbation of the equilibrium between crystal dissolution and growth may be engineered by introducing a small quantity of large crystals of one hand to a racemic slurry of crystals under deracemization conditions. This is shown in Figure 4. When a small quantity of large crystals of *R*-**1** was

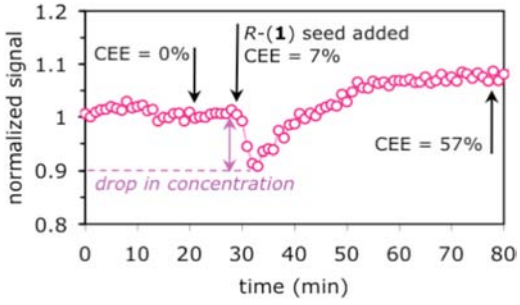

Figure 4. Normalized solution concentration of **1** as a function of time monitored by in situ FTIR spectroscopy for *rac*-**1** with DBU under enhanced attrition conditions. Seed crystals of *R*-**1** added at time shown to give solid-phase ee (%CEE) = 7%. Transient drop in solution concentration and evolution of CEE are shown.[16]

dx.doi.org/10.1021/ja303566g | J. Am. Chem. Soc. 2012, 134, 12629–12636

introduced into a racemic system under attrition enhanced conditions (ca. 2 wt %, to give an overall CEE of ca. 7% *R*-**1**), the solution concentration of **1** dropped immediately and rapidly by ca. 8%, followed by a slower recovery over time. Figure 4 shows that, concomitant with the drop in solution concentration, this seeding event resulted in a rapid evolution of solid-phase ee toward *R*-**1**, attaining 57% CEE measured 1 h after the seed crystals were added.[16]

The stochastic nature of the process is intriguing, and the parameters that control or trigger the crystal growth/broadening and the concomitant rapid evolution of solid-phase ee shown in Figures 1−3 are not well understood. Experiments carried out under what appear to be identical experimental conditions, resulting in homochirality in opposite senses in some cases and not at all in others, imply that whether crystals grow, and which enantiomorph will grow, depends both on possible minute initial asymmetry in mass or crystal size as well as on variability in the attrition process and is difficult to predict quantitatively for any particular attrition experiment.

Isotopic Labeling Studies. As a further probe of how attrition influences the reversible processes of molecule dissolution from and attachment to crystals, we designed experiments aimed at "tagging" molecules to monitor and deconvolute these mass transfer processes from the overall deracemization. Enantiopure compound **1** of both hands was synthesized with ^{15}N label at the amide nitrogen, as described in the Supporting Information, in order to monitor the physical movement of molecules between the solution and solid phases and in their conversion between the two enantiomorphic solids.

In a first set of experiments, saturated CH_3CN solutions of ^{14}N-*rac*-**1** were mixed with solid ^{15}N-*rac*-**1** to form a slurry. The reverse mixture was also prepared (isotopically ^{15}N-labeled **1** in solution phase). The mixtures were prepared such that the total mass of **1** in solution at the outset is approximately equal to the mass of **1** in the solid phase, such that the overall system contains an equal number of ^{14}N and ^{15}N molecules. Monitoring the isotopic label in each phase allows tracking of the net movement of molecules over time. Thus, upon complete mixing, the system will exhibit a ca. 50:50 mixture of ^{14}N/^{15}N in both solution and solid phases. The system was allowed to mix over time under *non*-racemizing conditions both with attrition by glass beads and without attrition, as illustrated in Figure 5 (top). The plot in Figure 5 (bottom) shows the physical movement of mass between solution and solid phases in the absence of the chemical influence of solution-phase racemization.

Solution- and solid-phase samples were acquired over time, and ^{14}N/^{15}N ratios were measured by high-resolution LC/MS integrating the ion patterns of the M^+H and M^+Na peaks.[16] Figure 5 shows that the mixing between phases is much more rapid under attrition conditions, with the labeled molecules being almost fully distributed between the two phases within 6 h. However, complete exchange of solution- and solid-phase molecules occurs over time under either mixing protocol.

These studies demonstrate that for systems undergoing attrition with glass beads, the complete exchange of mass between solid and solution phases under non-racemizing conditions occurs over a relatively short period of time. This suggests that crystals have been ablated to such an extent that all solid-phase molecules, even those at the very interior of crystals at the outset, have been exposed to the solution phase. This net movement of mass occurs on approximately the same time scale as the net conversion of one enantiomorph to the other under conditions where a racemization catalyst is present in the solution phase. Thus it is probable that each solid-phase molecule may have exchanged even multiple times with solution-phase molecules over the course of deracemization experiments such as those shown in Figure 1.

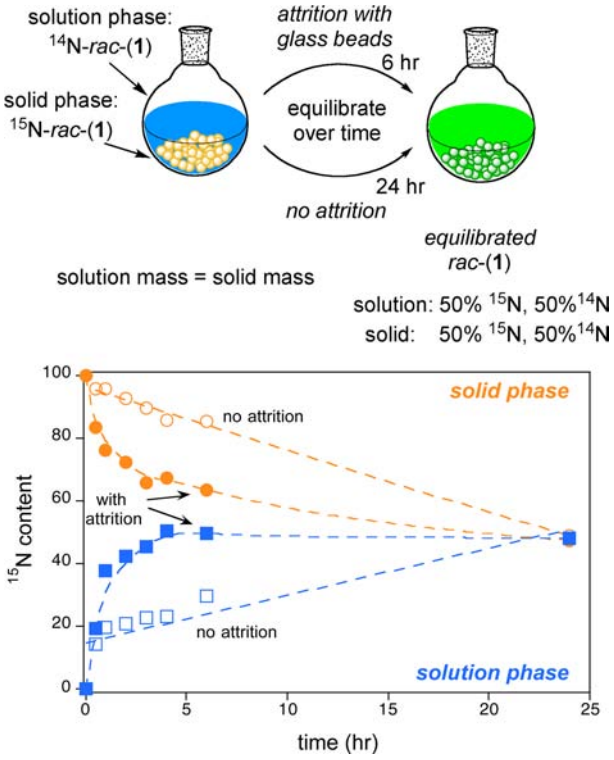

Figure 5. Monitoring ^{15}N content to follow mass transfer between solution (blue) and solid (gold) phases under nonracemizing conditions from the experiment shown (top) using isotopically labeled *rac*-**1**. Starting conditions: equal masses of ^{14}N-*rac*-**1** in solution and ^{15}N-*rac*-**1** in solid phase at outset. Graph shows ^{15}N content of *rac*-**1** molecules as they appear in the solution (blue symbols) and disappear from the solid (gold symbols) over time. Open symbols, no attrition; filled symbols, with attrition.[16] Dotted lines are given as a guide to the eye.

We next explored this movement of mass between solid and solution phases when it is accompanied by the other rate processes critical to attrition-enhanced deracemization, which include the chemical rate of interconversion between the enantiomers in solution and the net rate of conversion from one solid enantiomorph to the other. Experiments were carried out starting with racemic mixtures of enantiomorphic solids in saturated aqueous solution, with conditions as described in Figure 6 (top). In this set of experiments, one solid enantiomorph is comprised of molecules with the ^{15}N label and the other with ^{14}N. Thus, in the saturated solution at the outset of the experiment, all solution molecules of one enantiomer are labeled ^{14}N and the other enantiomer ^{15}N, as is the case for the solids. The vessel was subjected to sonication in the presence of glass beads, and the organic base DBU was then added, providing conditions identical to those of the experiments that were shown in Figure 1, where the racemization half-life in solution has been measured to be on the order of minutes. The solid phase was sampled over time and subjected to high-resolution chiral LC/MS to determine the ^{15}N content of each enantiomer.[16]

dx.doi.org/10.1021/ja303566g | *J. Am. Chem. Soc.* 2012, 134, 12629−12636

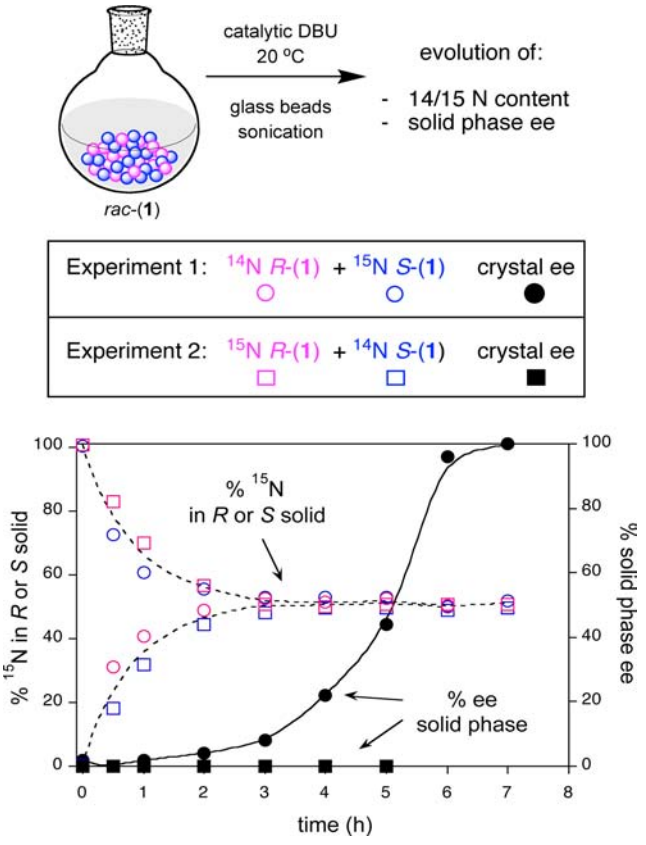

Figure 6. Percentage ^{15}N in *R* or *S* solid enantiomorph (open circles and squares) and solid-phase ee (filled circles and squares) as a function of time for two attrition-enhanced deracemization experiments carried out using initially racemic solids under conditions identical to those shown in Figure 1. Experiment 1 (circles): *S*-solid initially labeled with ^{15}N. Experiment 2 (squares): *R*-solid initially labeled with ^{15}N.[16]

The open symbols in the plot of Figure 6 (bottom, left axis) show that under the combined processes of solution racemization and sonication-attrition, the exchange of molecules between the two hands of the molecule and between the two solid enantiomorphs is rapid, reaching complete homogeneity within 3−4 h. In four separate experiments (two shown in Figure 6; all four shown in Figure 1), ^{15}N molecules from one enantiomorph dissolve into solution, convert to the opposite enantiomer, and attach to the other enantiomorph in a rapid, reversible, and reproducible manner.[20]

Interestingly, however, Figure 6 also shows that, while mass transfer occurs in a consistent manner, the *net* movement converting one solid enantiomorph to the other remains a random process, as indicated by the solid-phase ee. Homochirality emerged in one case while the other remained racemic. Of a total of four runs carried out using isotopically labeled racemic solids under these conditions, two achieved homochirality toward *S*-**1** and the other two remained racemic.[16] Thus, the physical and chemical exchanges of molecules in solution and solid phases cannot be correlated in a simple manner with the net movement of enantiomeric molecules from one solid enantiomorph to the other.

Taken together, these results demonstrate the ease with which molecules move between solution and solid phases under attrition-enhanced stirring or sonication, and at the same time they highlight the randomness of the overall *net* conversion from one solid enantiomorph to the other in the deracemization process. The results of Figures 1−4 show that the evolution of CEE commences concomitant with a transient crystal-size-induced solubility difference between the two enantiomorphs. The results in Figures 5 and 6 show that while the net solution−solid physical movement of molecules and the solution−solution chemical interconversion of enantiomers are facile processes, the stochastic manner in which an attrition-induced solubility difference is established makes it difficult to control or predict if and when such a crystal growth/solubility driving force will be sustained long enough for the evolution of solid-phase ee to commence.

Crystal-Size-Induced Solubility Driving Force. We reasoned that the process triggering the evolution of solid-phase ee would be reliably reproducible if a means could be found to maintain the crystal-size-induced solubility gradient. Sustaining a population of larger crystals of one of the enantiomorphs requires a reliable means of preventing their attrition, which is difficult to control in the presence of crystals of the other enantiomorph. This led to the idea of creating a physical separation between two solid-phase environments: one, a racemic slurry of crystals under attrition-enhanced solubility conditions, and two, a mildly stirred, lower solubility enantiopure "seed" population of single handedness in a separate vessel. The two vessels communicate without movement of solids, solely by circulation of the liquid phase between the vessels. A deracemization protocol based on this concept is illustrated in Figure 7.

In step 1 of Figure 7, a racemic mixture of crystals of compound **1** is stirred vigorously in the presence of glass beads in the left vessel, while a second pot containing a saturated solution of a small amount of *S*-**1** seed crystals is mildly stirred. The entire system is maintained at constant temperature, with solution-phase racemization and crystal-size-induced solubility differences being the sole driving forces for the net conversion of one solid enantiomorph to the other. Over time (ca. 16 h) and with circulation of only the liquid phase between the two vessels, the entire mass of *rac*-**1** is moved from the left-side vessel and converted to solid *S*-**1** in the right-side vessel, leaving only the glass beads and a saturated racemic solution behind in the left-side vessel.

In step 2 of Figure 7, glass beads are added to the vessel containing the mass of newly converted *S*-**1**, which is stirred vigorously with liquid circulation connecting it to a new vessel containing seeds of *R*-**1** that are mildly stirred in the absence of glass beads. In ca. 16 h this system is in turn fully converted from solid *S*-**1** in the right-hand vessel to solid *R*-**1** in the left-hand vessel. The procedure is repeated in step 3, where solid *R*-**1** is converted back to solid *rac*-**1**. The entire process is isothermal, with only dissolved molecules and no solids moving between the vessels. The interconversion between solid enantiomorphs relies solely on the differential enantiomer solubility induced by crystal size differences promoted by attrition in one vessel and mild stirring in the other vessel, as dictated by the Gibbs−Thomson rule, with solution racemization serving as the conduit between the two enantiomorphic solids.

The overall three-step process thereby converts *rac*-**1** to *rac*-**1** in 86% yield, with losses being due to sampling and to solid retention on the filters.[16] While the conversion of *rac*-**1** to *rac*-**1** is not a practically useful result, this experiment serves to demonstrate the remarkable ease with which a predictable crystal-size-induced solubility difference can drive the attrition-

dx.doi.org/10.1021/ja303566g | J. Am. Chem. Soc. 2012, 134, 12629−12636

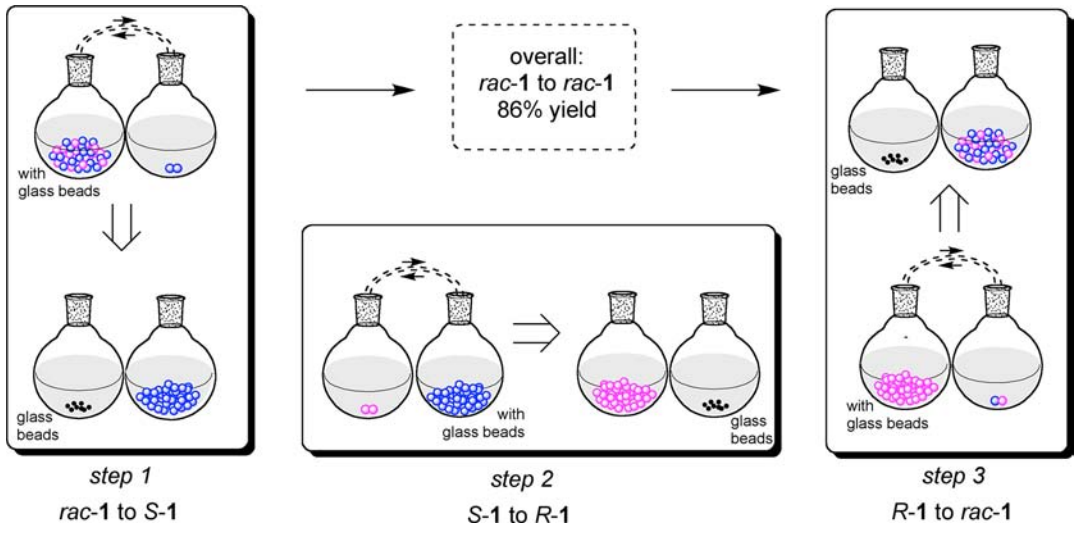

Figure 7. Schematic of iterative process of attrition-enhanced deracemization under solution-phase racemizing conditions (0.1 M DBU) in a two-vessel setup held under isothermal conditions at 20 °C. Solution phase is circulated between the left and right vessels at ca. 1 mL/min while movement of solids is prevented by 0.2 μm filters. Step 1: left vessel containing 200 mg of solid *rac*-**1** and glass beads in saturated CH_3CN solution is rapidly stirred, while right vessel containing 10 mg of seed crystals of *S*-**1** is mildly stirred. After ca. 24 h, *rac*-**1** solid was completely converted to *S*-**1** solid and was transferred to the right vessel via the solution phase, leaving only solution phase and glass beads in the vessel on the left. Step 2: glass beads are added to vessel containing *S*-**1** from step 1, which is connected to a new, mildly stirred vessel on the left containing 10 mg of seed crystals of *R*-**1**. After ca. 8 h, all solid was transferred to the left vessel via the solution phase and was completely converted to solid *R*-**1**. Step 3: glass beads are added to vessel containing *R*-**1** from step 2, which is connected to a new, mildly stirred vessel on the right containing 10 mg of seed crystals of *rac*-**1**. After ca. 24 h, all solid was transferred to the left vessel via the solution phase and was completely converted back to solid *rac*-**1**. The 86% overall solid-phase yield includes solid losses due to sampling and adherence to the filters.[16]

enhanced deracemization process in a controlled manner. This is in stark contrast to the stochastic nature of the process observed in the single-vessel protocol, where establishment of a transient crystal-size-induced solubility difference between enantiomorphs is correlated with the evolution of solid-phase ee. The protocol shown in Figure 6 utilizes this solubility driving force while eliminating the randomness observed in the one-pot deracemization.

Attrition-enhanced deracemization has typically been carried out using a small excess of one enantiomorph in order to provide a bias to help overcome the stochastic nature of the process. However, results showing that a slight bias in CEE can be overcome by a bias toward larger crystals of the opposite enantiomorph highlight the sensitive interplay between the driving forces presented by a population advantage and by a size advantage: a larger number of smaller crystals of one enantiomorph can be made to evolve to the opposite enantiomorph, which initially contained a smaller total number of molecules exhibiting a larger average crystal size. Experimental results to date demonstrating the success of "size over numbers" are limited to cases with a small initial bias, however, and certainly the conversion of an overwhelming population of one enantiomorph to what was initially only a few crystals of the other—the transformation shown in step 2 of Figure 7—is unprecedented in attrition-enhanced deracemization results reported to date.

From Deracemization to Resolution. The majority of chiral molecules that form enantiomorphic solids do not undergo solution racemization in a facile manner. For example, sodium ammonium tartrate **2**, the conglomerate system separated manually by Pasteur using tweezers,[20] does not racemize in the presence of acid or base. We envisioned that the concept of crystal-size-induced solubility differences might be extended to the *separation* of, rather than *conversion* between, enantiomers in such cases. Figure 8 demonstrates this protocol for an initially racemic mixture of enantiomorphic crystals of Pasteur's tartrate, **2**.

A flask containing equal amounts of solid sodium ammonium L- and D-tartrate crystals in a saturated aqueous solution together with 3 mm glass beads was connected to a second flask, with liquid circulation between the two vessels at ca. 1 mL/min, while the movement of solids was prevented by filters (Figure 8). To the second flask was added 50 mg of larger D-tartrate crystals. The flask containing crystals and beads was stirred vigorously while the second vessel was stirred only mildly. The system was held isothermally at 13 °C. Over time an increase in the amount of solid in the seed crystal vessel became apparent. The experiment was terminated at 60 h, and the solid phase in each vessel was collected, weighed, and dissolved in water for optical rotation measurements. The sample from the vessel originally containing an equal mixture of L and D crystals measured >98% ee L-tartrate, and the seed vessel, now containing more than an order of magnitude greater mass of crystals than at the outset, measured >99% ee D-tartrate. Solid mass recovery was ca. 70%, with losses due to sampling and adherence to the filters.[16]

Crystals from the attrition flask (Figure 8, left) exhibit much smaller average size than those collected from the seed flask (Figure 8, right), but both show the distinct hemihedral shape reported by Pasteur.[16] Mass transfer and growth of larger D crystals on the right occurs at the expense of the smaller, more readily dissolvable crystals undergoing attrition on the left. In the absence of primary nucleation of new L crystals in the right flask, only D molecules are able to add to the solid phase in the right flask. The success of the experiment indicates that primary nucleation is hindered by control of the level of supersaturation in the right flask. This net movement of mass via the liquid phase results ultimately in the quantitative physical separation

dx.doi.org/10.1021/ja303566g | J. Am. Chem. Soc. 2012, 134, 12629–12636

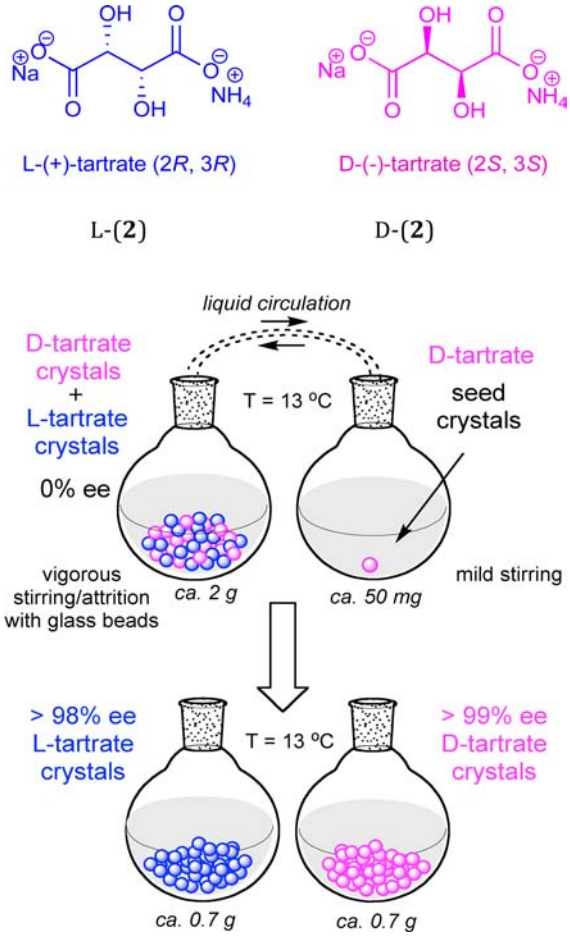

Figure 8. Extension of crystal-size-induced solubility driving force to the separation of non-racemizing conglomerate crystals.[16]

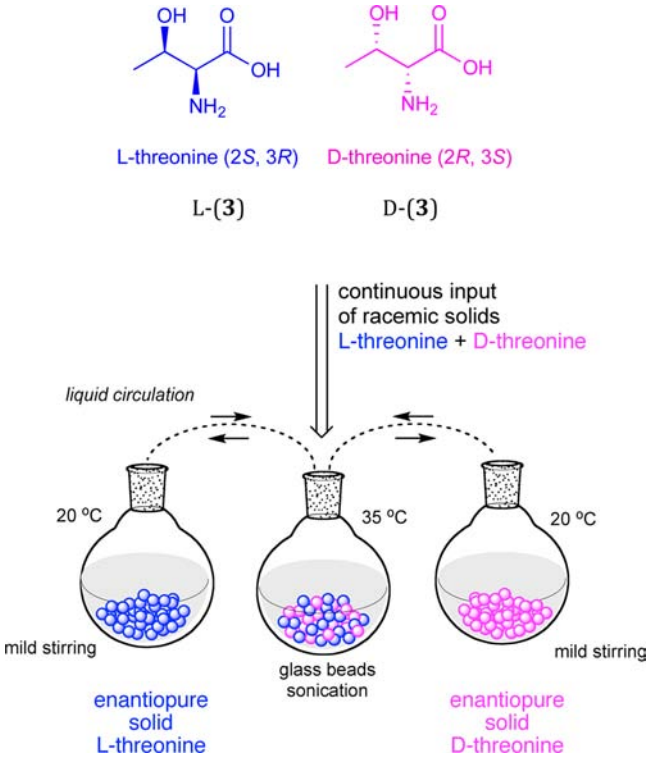

Figure 9. Extension of crystal-size-induced solubility driving force to the separation of non-racemizing conglomerate crystals, employing a temperature gradient and a continuous three-pot protocol.[16]

of the enantiomorphic crystals. A crystal-size-induced solubility gradient serves the role of Pasteur's tweezers.

A complementary means to establish solution concentration gradients for separation of enantiomers is to employ temperature programming as is typically carried out in preferential crystallization methods.[20,21] However, in many practical examples of non-racemizable conglomerates, the use of a temperature gradient to effect solubility differences may be problematic.[22] The attainment of equilibrium solubility conditions can be slow; a suitable, stable supersaturation zone may be difficult to identify; and primary nucleation of crystals of the wrong hand can become difficult to avoid, especially for highly concentrated solutions of highly soluble compounds. The crystal-size-induced solubility driving force may present a more reliable means of controlling the process than the use of temperature alone. A combination of temperature- and crystal-size-induced solubility driving forces may permit the resolution of difficult-to-resolve conglomerate systems. We demonstrated the combination of temperature- and crystal-size-induced solubility driving forces in this fashion for the proteinogenic amino acid threonine, **3**, which forms conglomerate solids and is not readily racemizable. Figure 9 demonstrates this case, together with a further practical modification of this protocol using a three-pot system.

Two mildly stirred vessels respectively containing seeds of D and L enantiomorphic solids of **3** at 20 °C are connected via a common circulating solution phase to a third pot containing a slurry of the racemic D and L solids under attrition conditions at 35 °C. The mass of each pure enantiomorphic solid builds up in the respective mildly stirred vessels while the racemic solid is depleted in the third vessel. Over the course of 48 h, *rac*-**3** was added to the central flask, allowing the process to operate in continuous fashion. Eight hours after stopping the central feed, no solids remained in the central vessel. Enantiopure L-**3** and D-**3** were isolated from the left and right receiver flasks in 76% and 79% yield, respectively, demonstrating a practical and efficient resolution of the enantiomorphic solids.[16]

In addition to the clear practical application to chiral separations demonstrated here, the concept of a crystal-size-induced solubility driving force may have implications for studies aimed at understanding the origin of biological homochirality. The concept of separation of conglomerate crystals has been discussed in this context since Pasteur's time. Welch[24] introduced the idea of "stochastic sorting", in which simple physical processes (wind and waves, coupled with rain and evaporation) might randomly partition crystals to create local regions of single chirality, even in a globally racemic environment. Upon dissolution of crystals from such regions, local pools of enantioenriched molecules might be formed, which could then undergo chemical reactions leading to molecules of higher complexity and sustainable enantioenrichment. However, in the absence of further driving forces to promote enantiomer separation, competing processes of re-equilibration to a locally racemic environment may be sufficient to hinder enantioenrichment. The crystal-size-induced solubility gradient acting as a separation driving force, as described in the current work, could enhance these simple stochastic sorting processes toward the establishment of regions exhibiting a single solid enantiomorph.

dx.doi.org/10.1021/ja303566g | J. Am. Chem. Soc. 2012, 134, 12629−12636

CONCLUSIONS

The results reported here help to deconvolute the various chemical and physical rate processes that occur during attrition-enhanced deracemization. Molecules move rapidly between the solution and solid phases under attrition conditions, on a time scale similar to that of the net conversion of one enantiomorphic solid to the other; yet the net evolution of crystal enantiomeric excess cannot be correlated in a simple manner with the phase transfer of molecules. A transient growth in crystal size is correlated with the accelerated evolution of solid-phase homochirality, and the stochastic nature of the process rationalizes the observed random outcomes of the deracemization process for initially racemic mixtures. The concept of a crystal-size-induced solubility driving force helps to define the mechanism and is exploited to develop a novel and reproducible approach for the separation of enantiomorphic solids. Implications for the emergence of single chirality in biological molecules are discussed.

ASSOCIATED CONTENT

Supporting Information

Details of general methods for synthesis and deracemization experiments, CSD measurements, ee measurement, and isotope measurements. This material is available free of charge via the Internet at http://pubs.acs.org.

AUTHOR INFORMATION

Corresponding Author

blackmond@scripps.edu

Notes

The authors declare no competing financial interest.

ACKNOWLEDGMENTS

D.G.B. acknowledges funding from the NSF (CBET Award 1066608) for the work on compounds **1** and **3** and NASA (Exobiology NNX12AD78G) for the work on Pasteur's tartrate **2**. Dr. William B. Kiosses (TSRI Core Microscopy) is acknowledged for assistance with light microscopy imaging and crystal population analysis.

REFERENCES

(1) Viedma, C. *Phys. Rev. Lett.* **2005**, *94*, 065504-1−065504-4.
(2) (a) van't Hoff, J. H. *Ber. Dtsch. Chem. Ges* **1902**, *35*, 4252−4264. (b) Roozeboom, H.W. B. *Z. Phys. Chem. Stoech Verwandt* **1899**, *28*, 494−517.
(3) (a) Kondepudi, D. K. *Science* **1990**, *250*, 975−976. (b) McBride, J. M.; Carter, R. L. *Angew. Chem., Int. Ed. Engl.* **1991**, *30*, 293−95.
(4) Noorduin, W. L.; Izumi, T.; Millemaggi, A.; Leeman, M.; Meekes, H.; Van Enckevort, W. J.; Kellogg, R. M.; Kaptein, B.; Vlieg, E.; Blackmond, D. G. *J. Am. Chem. Soc.* **2008**, *130*, 1158−1159.
(5) Viedma, C.; Ortiz, J. E.; de Torres, T.; Izumi, T.; Blackmond, D. G. *J. Am. Chem. Soc.* **2008**, *130*, 15274−15275.
(6) Crusats, J.; Veintemillas-Verdaguer, S.; Ribo, J. M. *Chem.—Eur. J.* **2006**, *12*, 776−7781.
(7) Viedma, C. *Astrobiology* **2007**, *7*, 312−319.
(8) Blackmond, D. G. *Chem.—Eur. J.* **2007**, *13*, 3290−3295.
(9) McBride, J. M.; Tully, J. C. *Nature* **2008**, *452*, 161−162.
(10) Leeman, M.; de Gooier, J. M.; Boer, K.; Zwaagstra, K.; Kaptein, B.; Kellogg, R. M. *Tetrahedron: Asymmetry* **2010**, *21*, 1191−1193.
(11) (a) Noorduin, W. L.; van der Asdonk, P.; Bode, A. A.; Meekes, H.; Van Enckevort, W. J.; Vlieg, E.; Kaptein, B.; van der Meijden, M.; Kellogg, R. M.; Deroover, G. *Org. Process Res. Dev.* **2010**, *14*, 908−911. (b) Maarten, W.; van der Meijden, M.; Leeman, M.; Gelens, E.; Noorduin, W. L.; Meekes, H.; van der Enckevort, W. J.; Kaptein, B.; Vlieg, E.; Kellogg, R. M. *Org. Process Res. Dev.* **2009**, *13*, 1195−1198.
(12) (a) Noorduin, W. L.; Bode, A. A.; van der Meijden, M.; Meekes, H.; van Etteger, A. F.; van Enckevort, W. J.; Christianen, P. C.; Kaptein, B.; Kellogg, R. M.; Rasing, T.; Vlieg, E. *Nature Chem.* **2009**, *1*, 729−732. (b) Noorduin, W. L.; Meekes, H.; van Enckevort, W. J.; Millemaggi, A.; Leeman, M.; Kaptein, B.; Kellogg, R. M.; Vlieg, E. *Angew. Chem., Int. Ed.* **2008**, *47*, 6445−6447. (c) Kaptein, B.; Noorduin, W. L.; Meekes, H.; van Enckevort, W. J.; Kellogg, R. M.; Vlieg, E. *Angew. Chem., Int. Ed.* **2008**, *47*, 7226−7229. (d) Noorduin, W. L.; van Enckevort, W. J.; Meekes, H.; Kaptein, B.; Kellogg, R. M.; Tully, J. C.; McBride, J. M.; Vlieg, E. *Angew. Chem., Int. Ed.* **2010**, *49*, 8435−8438.
(13) Meekes, H.; Noorduin, W. L.; Bode, A. A. C.; van Enckevort, W. J. P.; Kaptein, B.; Kellogg, R. M.; Vlieg, E. *Cryst. Growth Des.* **2008**, *8*, 1675−1681.
(14) (a) Uwaha, M. *J. Phys. Soc. Jpn.* **2004**, *73*, 2601. (b) Skrdla, P. *Cryst. Growth Des.* **2011**, *11*, 1957−1965.
(15) Iggland, M.; Mazzotti, M. *Cryst. Growth Des.* **2011**, *11*, 4611−4622.
(16) See Supporting Information for details.
(17) The presence of chiral impurities was in fact invoked to help rationalize the apparent *lack* of randomness in results that appeared skewed toward one enantiomorph in the first report of attrition-enhanced deracemization of intrinsically chiral molecules (see ref 4).
(18) The experiments of Figure 2 were carried out with ca. 300 mg of *rac*-**1** in 3 mL of MeCN, of which ca. 250 mg remains in the solid phase. Thus, for series b and series c, the evolution to homochirality that takes place over 2 h between the 3 and 5 h sampling points involves the conversion of ca. 125 mg of one enantiomorph to the other, for an average mass conversion rate of ca. 1 mg/min.
(19) Samples were imaged on a laser scanning confocal microscope to produce high-resolution snapshots of 5−7 randomly selected regions (for a population size of 11 000−17 000 individual particles) for each sample. A calibrated perimeter around each crystal defined in 2D space is created by the imaging software to generate a total count of individual objects with area expressed in μm^2. Results are sorted into histograms reporting fraction of total crystal area as a function of the bins of crystal area range in μm^2.
(20) The question of kinetic isotope effects in the use of ^{15}N-**1** in tracking the movement of molecules should be addressed. In the four experiments conducted under the conditions shown in Figure 5, the two that evolved to single chirality in *S*-**1** were initiated in one case with the ^{15}N tag present in the *S*-**1** solid and in the other case with the ^{15}N tag in the *R*-**1** solid. Similarly, the two that remained racemic commenced with the ^{15}N tag in opposite enantiomorphs. These results imply the absence of any kinetic isotope effects in the deracemization process.
(21) Pasteur, L. C.R. *Hebd. Séanc. Acad. Sci. Paris* **1848**, *26*, 535−538.
(22) Jacques, J.; Collet, A.; Wilen, S. H. *Enantiomers, Racemates and Resolution*; Krieger: Florida, 1994; Chap. 4.
(23) Levilain, G.; Coquerel, G. *CrystEngComm* **2010**, *12*, 1983−1992.
(24) Welch, C. R. *Chirality* **2001**, *13*, 425−427.